

# Boundary conditions at the mobility edge

D. Braun<sup>1</sup>, G. Montambaux<sup>2</sup> and M. Pascaud<sup>2</sup>

<sup>1</sup> Universität-Gesamthochschule Essen, Fachbereich 7 - Physik, 45117 Essen, Germany

<sup>2</sup> Laboratoire de Physique des Solides, associé au CNRS

Université Paris-Sud, 91405 Orsay, France

February 1, 2008

It is shown that the universal behavior of the spacing distribution of nearest energy levels at the metal-insulator Anderson transition is indeed dependent on the boundary conditions. The spectral rigidity  $\Sigma^2(E)$  also depends on the boundary conditions but this dependence vanishes at high energy  $E$ . This implies that the multifractal exponent  $D_2$  of the participation ratio of wave functions in the bulk is not affected by the boundary conditions.

PACS numbers: 72.15.Rn, 73.23.-b, 05.45.+b

The spectral analysis of disordered conductors has been proven recently to be a useful tool to probe the nature of the eigenstates [1,2,3,4]. In the diffusive (metallic) regime, the conductance  $g$  scales linearly with the size  $L$  of the system, and the wave functions are delocalized over the sample. The spectral correlations have been shown to be those of random gaussian matrices [5], with large deviations above the Thouless energy  $E_c = \hbar/\tau_D = \hbar D/L^2$  [6], where  $D$  is the diffusion coefficient and  $\tau_D$  is the time needed for a wave packet to cross the sample. In particular, the distribution  $P(s)$  of spacings between nearest levels is very well fitted by the Wigner-Surzize characteristic of chaotic systems [7]:  $P(s) = (\pi/2)s \exp[-(\pi/4)s^2]$  where  $s$  is written in units of mean level spacing  $\Delta$  [8]. These deviations of order  $1/g^2$  [9] become negligible in the limit of large  $L$ . In the localized phase, in the limit  $L \rightarrow \infty$ , the levels become completely uncorrelated and  $P(s)$  has the poissonian form:  $P(s) = \exp(-s)$ . This is because two levels close in energy are distant in space so that their wave functions do not overlap.

It has been found that the Anderson metal-insulator transition in three dimensions is characterized by a third distribution [1] which has the remarkable property to be universal, i.e. it is independent of the size, whereas it is size dependent in the localized and metallic regimes. The transition is thus described as an unstable fixed point, in the sense that slightly above the transition ( $W > W_c$ , where  $W$  is the disorder strength and  $W_c$  is the critical disorder) the distribution tends to a poissonian limit when  $L \rightarrow \infty$ , while slightly below the transition ( $W < W_c$ ), it tends to the Wigner-Dyson (WD) distribution. This third universal distribution has been extensively studied by several groups who confirmed these results, for  $L$  ranging from 6 to 100 [10,12,13,14,15,16,17]. Up to now, the form of the distribution is still unexplained.

$P(s)$  carries information on the short range part of the spectral correlations. Other characterizations are the two-level correlation function (TLCF) of the density of

states  $\rho(\epsilon)$ :  $K(s) = \langle \rho(\epsilon + s)\rho(\epsilon) \rangle / \langle \rho(\epsilon) \rangle^2 - 1$  and the so-called number variance  $\Sigma^2(E) = \langle N^2(E) \rangle - \langle N(E) \rangle^2$  which measures the fluctuation of the number of levels  $N(E)$  in a band of width  $E$ .  $E$  is in units of  $\Delta$ . It is related to the TLCF:  $\Sigma^2(E) = 2 \int_0^E (E - s)K(s)ds$ . Surprisingly enough, the numerical studies which lead to the same shape of the distribution  $P(s)$  at the transition have apparently been all performed using *periodic boundary conditions*. In this work, we have calculated  $P(s)$  at the transition for the same hamiltonian, *with different boundary conditions* (BCs). The hamiltonian is taken as:

$$H = \sum_i \varepsilon_i c_i^+ c_i - t \sum_{(i,j)} (c_i^+ c_j + c_j^+ c_i). \quad (1)$$

The sites  $i$  belong to a 3D cubic lattice. Only transfer  $t$  between nearest neighbours  $(i,j)$  is considered. The site energies  $\varepsilon_i$  are chosen independently from a symmetric box distribution of width  $W$ . The metal-insulator transition occurs at the center of the band for the critical value  $W_c = 16.5 \pm .2$  [1,11,12,14]. We have found that *although the level statistics at the transition is independent of the size of the system, it depends on the boundary conditions*. Our main result is shown in Fig.1 where we have plotted the spacing distribution for four types of BCs, a) periodic in the three directions (the situation studied by previous authors and that we will refer to as (111), b) periodic in two directions and "Hard Wall" (HW) (Dirichlet) in the third (110), c) periodic in one direction and HW in the two others (100), d) HW in the three directions (000). All these distributions are "universal" in the sense that they are size independent. The critical point depends at most very weakly on the choice of the BCs. It seems to shift slightly to smaller  $W$  when the number of HW boundaries is increased. Using standard scaling analysis of  $\langle s^2 \rangle$  and  $\int_0^2 P(s) ds$ , we found  $W_c = 16.0 \pm .5$  for the (000) geometry. However, within the range of sizes studied ( $L = 12, \dots, 22$ ) the difference between the  $P(s)$  at  $W = 16.0$  and at  $W = 16.5$  is negligible compared to the remaining statistical fluctuations of the spacing

distribution.

In Fig.2 we have plotted the second moment of the level spacing  $\langle s^2 \rangle$  as a function of the size for the different BCs. This plot shows that the distributions are size independent and that they do not converge to a single one in the large size limit.

It may appear *a priori* surprising that the distribution is at the same time size independent and sensitive to the BCs. To clarify this point, it is instructive to recall the behavior of the typical dimensionless curvature  $g_d = \pi \langle |c| \rangle / \Delta$  of the energy levels when an infinitesimal flux is introduced in the cylinder geometry. In the metallic regime,  $g_d(L)$  increases linearly with the size and it decreases exponentially in the localized regime. At the transition, the curvature  $g_d(L) = g_d^*$  is size independent [18,19]. Since  $g_d$  measures the sensitivity of energy levels to a change of the BCs, the simple fact that it is non-zero shows that the spectral correlations can be at the same time size independent and sensitive to the BCs. This universal sensitivity to the BC has already been discussed in the case of *periodic BCs* where one or several Aharonov-Bohm (AB) fluxes were applied [20,21]. However in that case, the symmetry — time reversal invariance — was at the same time broken by the fluxes, such that it is not surprising that the statistics is changed.

The distribution found by other authors with periodic BCs is the most rigid of the four distributions that we have studied. When periodic BCs are relaxed and replaced by hard wall BCs, the distribution becomes closer to the Poisson distribution, with a short range repulsion which is characterized by a larger slope of  $P(s)$ . The slope  $P'(0)$  varies by more than a factor three from 2.14 [1] for the BC (111) to 6.80 for the BC (000) (see table I).

It is useful to stress that in the metallic regime itself, there are deviations to the WD distribution which depend on the BCs. These deviations are related to a contribution of the diffusive modes [9]. At small  $s$ , the slope of  $P(s)$  is given by

$$P(s) = \frac{\pi^2}{6} \left(1 + \frac{3a}{\pi^6 g^2}\right) s, \quad (2)$$

where the coefficient  $a$  describes the diffusive motion and is given by

$$a = \frac{\pi^4}{L^4} \sum_{q \neq 0} \frac{1}{(\mathbf{q}^2)^2}. \quad (3)$$

For an isolated system, the diffusion modes are quantized by the BCs. In a direction where the boundaries are hard walls,  $q = n\pi/L$  with  $n = 0, 1, 2, 3, \dots$ . In a direction where the boundaries are periodic,  $q = 2n\pi/L$  with  $n = 0, \pm 1, \pm 2, \pm 3, \dots$ . In  $d = 3$ , one finds:  $a_{111} = 1.03$ ,  $a_{110} = 2.15$ ,  $a_{100} = 3.39$ ,  $a_{000} = 5.13$ . So in a metal, the slope of  $P(s)$  depends on the BC. However,

the corrections are order  $1/g^2$  and decrease with the size since  $g(L) \sim L$ , and they vanish for the infinite system. At the transition  $g = g^*$  is size independent and one may expect that the correction to  $P(s)$  still depends on the BC through the quantization of the anomalous diffusion modes. This correction can be also simply calculated for an anisotropic system. It depends on the shape of the sample. This certainly means that the spectral correlations at the transition are also shape dependent [22].

The distributions we have found bear an interesting similarity with another recently studied distribution [23]. A remarkable and simple spectral sequence which is intermediate between the WD and the Poisson distributions is obtained by taking the middles of a poissonian sequence. This new sequence has been baptized “semi-Poisson” [23]. The corresponding  $P(s)$  is given by [23,24]:

$$P(s) = 4s e^{-2s}. \quad (4)$$

It has been shown that the equilibrium distribution of charges in a Coulomb gas with logarithmic interaction only between *nearest neighbors* is also described by eq.(4). The TLCF and  $\Sigma^2(E)$  for this model (referred to later as Short Range Plasma Model, SRPM) are however different from those for the semi-Poisson sequence. We shall return to this point later.

In the inset of Fig.3 we have plotted the arithmetic average of the four distributions. Quite amazingly, it is very close to the semi-Poisson distribution. The average of the slope at small separation calculated with the four BCs is  $4.08 \pm 0.4$  instead of 4 for the semi-Poisson. As another characteristic of  $P(s)$ , the second moment  $\langle s^2 \rangle$  is shown in table I for the various BCs. The average over the different BCs is found to be  $1.51 \pm 0.01$ . It is  $3/2$  for the semi-Poisson. The tails of  $P(s)$  have also been considerably studied [1,3,4,13,15,17]. The inset of Fig.1 shows the tails for the four BCs. They clearly differ by the rapidity of their decay, the usual periodic BCs giving rise to the fastest decay. It is interesting to notice that the behavior at large  $s$  is much more affected by HW BCs than by a simple addition of a AB flux or even a magnetic field [20].

We have also investigated random boundary conditions, with random hopping terms  $t_{ij} = t_{ji}$  connecting opposite sides of the sample. Drawing the  $t_{ij}$  for each disorder realization independently from a box distribution centered around zero and with width  $\tau$ , we found a continuous family of “universal” critical ensembles, which are for finite  $\tau$  distinct from the ones with “deterministic” boundary conditions.

We now turn to the number variance. A linear behavior at large  $E$ ,  $\Sigma^2(E)/E \rightarrow \chi$  defines the level compressibility  $\chi$ , which is also related to the  $t \rightarrow 0$  dependence of the form factor  $\tilde{K}(t)$ , the Fourier transform of  $K(s)$ . One has  $\chi = \int_{-\infty}^{\infty} K(s) ds = \tilde{K}(0)$ . This means  $\chi = 1$  for the Poisson and semi-Poisson sequences,  $\chi = 0$  for the WD correlations and  $\chi = 1/2$  for the SRPM.

In Fig. 4, we have plotted  $\Sigma^2(E)/E$  for the various BCs. It is seen that, like for  $P(s)$ , the rigidity depends on the BCs for small energy ranges. The rigidity is weaker for non-periodic BCs. However, when  $E$  increases, the different rigidities seem to converge towards the same value (see inset of fig.4). We find  $\chi \simeq 0.27 \pm 0.02$  in agreement with previous authors [10,25]. Within error bars, this asymptotic value does not depend on the BCs.

$P(s)$  and  $\chi$  carry information on different time scales in the problem. Let us remind that the metallic spectrum is characterized by two characteristic time scales, the Thouless time  $\tau_D$  and the Heisenberg time  $\tau_H = h/\Delta$ , with  $\tau_H/\tau_D = 2\pi E_c/\Delta \gg 1$ . At the transition, these two times are of the same order. Consequently, correlation functions like  $P(s)$  which probe correlations at energy scales of the order of  $\Delta$ , i.e. time scales of the order of  $\tau_H \simeq \tau_D$ , probe the sensitivity to the boundary conditions of a wave packet evolution. However, the asymptotic form of the spectral rigidity at energy  $E \gg \Delta$  typically probes time scales  $t \ll t_H \simeq \tau_D$  for which the diffusion of a wave packet is insensitive to the BCs.

More precisely, the form factor has been shown to be related to the return probability  $P(t)$  for a wave packet [26,27]. At the transition, the wave functions have a multifractal structure [28,29], with a long range tail showing a power law decay. Multifractality is characterized by the time dependence, when  $t \ll \tau_D$ :

$$P(t) \propto t^{-D_2/d}, \quad (5)$$

where  $D_2$  is the multifractal exponent of the inverse participation ratio,  $\sum_{\mathbf{r}} \langle |\psi_n(\mathbf{r})|^4 \rangle \propto L^{-D_2}$  [28]. From the limit  $t \rightarrow 0$  of  $P(t)$ ,  $\chi$  is found to be [27]:

$$\chi = \frac{1}{2} \left( 1 - \frac{D_2}{d} \right).$$

The multifractal exponent  $D_2$  defined from small time behavior is thus expected to be independent of the BCs. Therefore  $\chi$  should not depend on the BCs either. This is seen to be true from the inset of fig. 4, where we show that  $\Sigma^2(E)/E$  converges to the same value  $\chi \simeq 0.27 \pm 0.02$  for periodic and HW BCs. This value of  $\chi$  leads to a multifractal exponent  $D_2 \simeq 1.4 \pm 0.2$  which has to be compared with the value  $D_2 \simeq 1.6 \pm .3$  found from other direct numerical calculations involving the study of the wave functions [30].

In conclusion, we have shown that the spectral correlations at the metal-insulator transition, although being universal, i.e. independent of the size, strongly depend on the choice of the boundary conditions. This dependence is most pronounced for small energy scales. When the periodic BCs are replaced by hard walls in one or more directions, the spectrum becomes less and less rigid. However, the level compressibility defined from the  $E \rightarrow \infty$  limit of the spectral rigidity is independent of the choice of the boundaries.

We acknowledge stimulating discussions with E. Bogomolny, V. Falko, I. Lerner, F. Piéchon, and P. Walker. Numerical simulations have been performed using IDRIS facilities (Orsay). G. M. thanks the Isaac Newton Institute for Mathematical Sciences for hospitality during the completion of this work.

	Wigner	111	110	100	000	SRPM	Poisson
$P'(0)$	$\frac{\pi^2}{6} = 1.65$	2.14 <sup>(2)</sup>	3.01	4.37	6.80	4	$\infty$
$\langle s^2 \rangle$	$\frac{4}{\pi}^{(1)} = 1.27$	1.41 <sup>(3)</sup>	1.48	1.55	1.62	3/2	2

Table I : Numerical results for the various measures of spectral correlations compared with the SRPM. The relative errors (standard deviations from 6 system sizes,  $L = 12, 14, 16, 18, 20, 22$ ; 500 to 33 disorder realisations) for  $B$  are always less than 10% and for  $s^2$  less than 1%.

<sup>(1)</sup> This is the value deduced from the Wigner surmise;

<sup>(2)</sup> See also ref. [1]; <sup>(3)</sup> See also ref. [15].

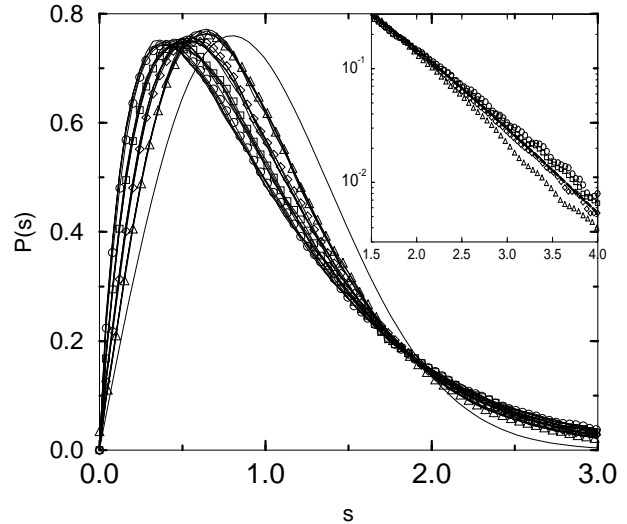


FIG. 1. Distribution  $P(s)$  at the metal-insulator transition with four different types of boundary conditions defined in the text:  $\triangle$  111,  $\diamond$  110,  $\square$  100, and  $\circ$  000. Distributions with  $L = 8$  to  $L = 14$  are shown. The Wigner-Dyson result (continuous line) is also plotted. In the inset the tails of  $P(s)$  are shown for  $L = 10$  and compared with the Semi-Poisson distribution, eq.(4) (dashed line).

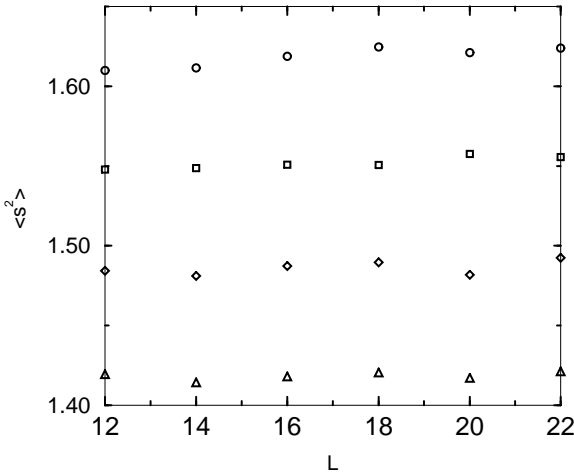


FIG. 2.  $\langle s^2 \rangle$  versus linear size  $L$  for different BCs (symbols as in Fig.1) for  $W = 16.5$ .

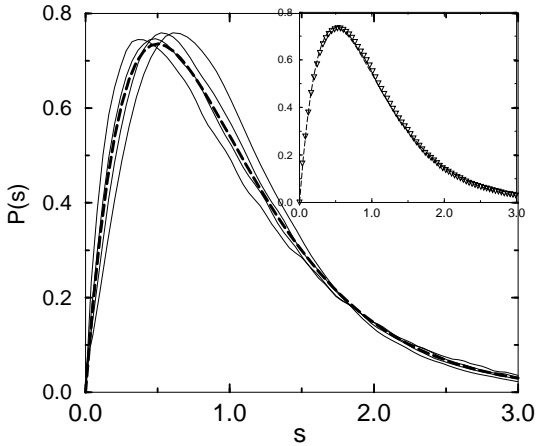


FIG. 3.  $P(s)$  for the four different BCs compared with semi-Poisson (dashed line). Inset: "Average"  $P(s)$  at the transition ( $\nabla$ ), compared with semi-Poisson.

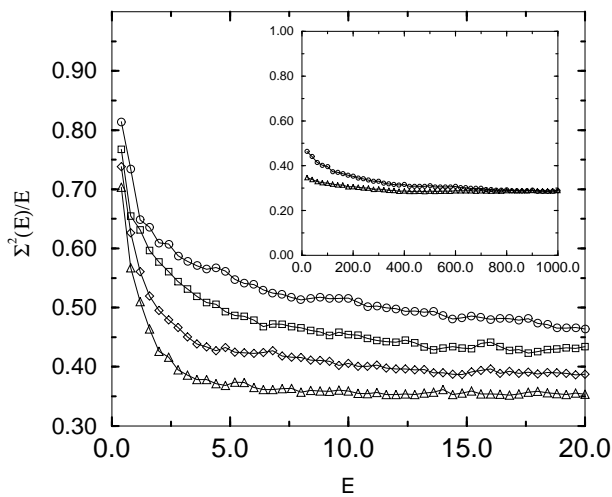


FIG. 4.  $\Sigma^2(E)/E$  for the different BCs (average over  $L = 20$  and  $22$ ). Symbols as in Fig.1. The inset shows that at large energy the difference between the BCs (111) and (000) vanishes.

---

[1] B.I. Shklovskii *et al.*, Phys. Rev. B **47**, 11487 (1993).  
[2] V.E. Kravtsov *et al.*, Phys. Rev. Lett. **72**, 888 (1994).  
[3] A.A. Aronov *et al.*, JETP Lett. **59**, 40 (1994); Phys. Rev. Lett. **74**, 1174 (1995).  
[4] V. Kravtsov and I. Lerner, J. Phys. A **28**, 3623 (1995).  
[5] K.B. Efetov, Adv. Phys. **32**, 53 (1983).  
[6] B.L. Alt'shuler and B. Shklovskii, Zh. Eksp. Teor. Fiz. **91**, 220 (1986) [Sov. Phys. JETP **64**, 127 (1986)].  
[7] M.L. Mehta, "Random Matrices", second edition, Academic Press, New York, 1991.  
[8] This simple surmise derived for a  $N \times N$  random matrix with  $N = 2$  is a rather good approximation of the  $N = \infty$  result. The slope at the origin is  $\pi^2/6$  for  $N = \infty$ .  
[9] V. Kravtsov and A. Mirlin, Pis'ma v ZhETF **60**, 656 (1994).  
[10] B.L. Alt'shuler *et al.*, JETP **67**, 625 (1988).  
[11] B. Kramer and A. MacKinnon, Rep. Prog. Phys. **56**, 1469 (1994).  
[12] E. Hofstetter and M. Schreiber, Phys. Rev. B **48**, 16979 (1993); Phys. Rev. B **49**, 14726 (1994).  
[13] S. Evangelou, Phys. Rev. B **49**, 16805 (1994).  
[14] I. Zharekeshev and B. Kramer, Phys. Rev. B **51**, 17239 (1995).  
[15] I. Varga *et al.*, Phys. Rev. B **52**, 7783 (1995).  
[16] D. Braun and G. Montambaux, Phys. Rev. B **52**, 13903 (1995).  
[17] I. Zharekeshev and B. Kramer, Phys. Rev. Lett. **79**, 717 (1997).  
[18] C.M. Canali *et al.*, Phys. Rev. B **54**, 1431 (1996).  
[19] D. Braun *et al.*, Phys. Rev. B **55**, 7557 (1997). The definition of  $g$  in this paper differs by a factor  $2\pi$ .  
[20] M. Batsch *et al.*, Phys. Rev. Lett. **77**, 1552 (1996).  
[21] G. Montambaux, Phys. Rev. B **55**, 12833 (1997).  
[22] During the revision of this paper, we have been aware that a recent work has reached this conclusion, H. Potempa and L. Schweitzer, cond-mat/9804312  
[23] E. Bogomolny *et al.*, preprint.  
[24] M. Pascaud and G. Montambaux, unpublished  
[25] I. Zharekeshev and B. Kramer, in "Quantum Transport in submicron structures", H.A. Cerdeira, B. Kramer and G. Schön (eds) NATO ASI Series E, **291**, 93 (1994).  
[26] N. Argaman *et al.*, Phys. Rev. B **47**, 4440 (1993).  
[27] J.T. Chalker *et al.*, Phys. Rev. Lett. **77**, 554 (1996); JETP Lett. **64**, 386 (1996).  
[28] C. Castellani and L. Peliti, J. Phys. A **19**, L429 (1986).  
[29] M. Schreiber, Phys. Rev. B **31**, 6146 (1985); M. Schreiber and H. Grussbach, Phys. Rev. Lett. **67**, 607 (1991).  
[30] For a review and recent calculations, see T. Brandes *et al.*, Ann. Phys. **5**, 633 (1996) and T. Ohtsuki and T. Kawarabayashi, cond-mat/9701013